On the survivability of planets in young massive clusters and its implication of planet orbital architectures in globular clusters

Cai, X.; Portegies Zwart, S.F.; Kouwenhoven, M.B.N.; Spurzem, R.

MNRAS **000**, 1–10 (2019) Preprint 7 March 2019 Compiled using MNRAS LATEX style file v3.0

On the survivability of planets in young massive clusters

Maxwell X. Cai[1⋆], S. Portegies Zwart[1], M.B.N. Kouwenhoven[2], Rainer Spurzem[3,4,5]
[1] *Leiden Observatory, Leiden University, PO Box 9513, 2300 RA, Leiden, The Netherlands*
[2] *Department of Mathematical Sciences, Xi'an Jiaotong-Liverpool University, 111 Ren'ai Rd., Suzhou Dushu Lake Science and Education Innovation District, Suzhou Industrial Park, Suzhou 215123, P.R. China*
[3] *National Astronomical Observatories and Key Laboratory of Computational Astrophysics, Chinese Academy of Sciences, 20A Datun Road, Chaoy*
[4] *Kavli Institute for Astronomy and Astrophysics, Peking University, 5 Yi He Yuan Road, Haidian District, Beijing 100871, P.R. China*
[5] *Zentrum für Astronomie, Astronomisches Rechen-Institut, University of Heidelberg, Mo ÌĹnchhofstrasse 12-14, D-69120 Heidelberg, Germany*

Accepted XXX. Received YYY; in original form ZZZ

ABSTRACT

As of March 2019, there is only one exoplanet among nearly 4000 confirmed exoplanets detected in dense GCs. Young massive Star clusters (YMCs) are widely considered as the progenitor of globular clusters (GCs). Motivated by the lack of planet detections in GCs, we use direct N-body simulations to study the survivability of planets in young massive clusters, and thereby constrain the probability that GCs inherit planets from YMCs. We conclude that most wide-orbit planets ($a \geq 20$ au), should they form in a YMC similar to Westerlund-1, will be ejected on a timescale of 10 Myr. Consequently, a majority of surviving exoplanets will have semi-major axes smaller than 20 au. Ignoring planet-planet scattering and tidal damping, the survival probability as a function of initial semi-major axis in au can be described as $f_{\rm surv}(a_0) = -0.33\log_{10}(a_0)+1$. About 28.8% of free-floating planets (FFPs) have sufficient speeds to escape from the host YMC at a crossing timescale upon their ejection. The other FFPs will remain bound to the cluster potential, but the subsequent mass segregation process could cause their delayed ejection from the host cluster during its course to evolve into a GC. As such, we expect that GCs are rich in short-period terrestrial planets, but are deprived of FFPs due to dynamical instability and Jovian planets due to the planet-metallicity correlation.

Key words: methods: numerical – planets and satellites: dynamical evolution and stability – planets and satellites: formation – galaxies: star clusters: general – globular clusters: general.

1 INTRODUCTION

Young massive star clusters (YMCs) are dense stellar systems of $\geq 10^4 M_\odot$, and with a typical age of just a few Myr (Portegies Zwart et al. 2010; Longmore et al. 2014). Due to their young ages, a significant fraction of gas content is still presented inside the cluster, and the star formation process is likely to be ongoing. Recent studies suggest that YMCs could be the progenitors of their older cousins, i.e., the long-lived globular clusters (GCs) (e.g., Kruijssen 2014). In this sense, the formation and early evolution history of GC member stars can be inferred from YMC member stars.

On the other hand, star formation is typically followed by planet formation (e.g., Fedele et al. 2010). It is now widely accepted that planets are prevalent in the universe (Winn & Fabrycky 2015). If YMCs are active environments for both star formation and planet formation, will GCs be able to inherit planet from YMCs? In other word, will the GCs be a place to hunt for planets?

Observationally, while the exoplanets encyclopedia records nearly 4,000 confirmed exoplanets as of March 2019, only fewer than 1% of these are detected in star clusters (see Table 1). The exoplanets detected in star clusters are plotted in Fig. 1 against exoplanets detected outside star clusters. Apart from the difference in numbers, planets detected inside and outside star clusters seems to be statistically indistinguishable, with the exception that the upper most point to the right representing PSR B1620-26 b (see Table 1) is probably formed by a dynamical interaction (Ford et al. 2000; Sigurdsson et al. 2003) in the dense core of Messier 4. The low number of planet detection in star clusters seems to be contradictory to the theoretical expectation (Lada & Lada 2003). The search of planets in dense star clusters started in from the late 1990s, when researchers use the

⋆ E-mail: cai@strw.leidenuniv.nl (MXC)

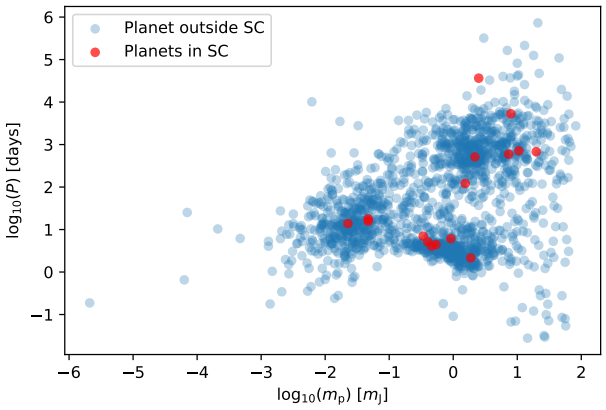

Figure 1. The masses (in Jupiter mass M_J) and orbital periods (in days) of planets inside/outside star clusters. Only confirmed planets with well-determined masses and orbital periods are shown. Exoplanet data downloaded from `exoplanet.eu` on 5 March 2019.

Hubble Space Telescope to observe the 47 Tucanae cluster for 8.3 days. No planet is detected despite that the cluster has 33,000 stars (Gilliland et al. 2000; Masuda & Winn 2017). It is certainly possible that observational biases are responsible, but various analysis on planets in star clusters (e.g., Adams et al. 2006; Malmberg et al. 2007; Proszkow & Adams 2009; Spurzem et al. 2009; Malmberg et al. 2011; Parker & Quanz 2012; Hao et al. 2013; Li & Adams 2015; Cai et al. 2017, 2018; van Elteren et al. 2019) have demonstrated that the dense star cluster environments have implication to the formation and evolution of planets.

One could roughly divide the entire formation and evolution history of planets in star clusters, as shown in Fig 2. Planetary systems may be influenced by their birth environments in the following ways: first, during the planet formation process (Phase 1), protoplanetary disks may be photo-evaporated due to the possible presence of nearby OB stars (e.g., Störzer & Hollenbach 1999; Armitage 2000; Adams 2010; Anderson et al. 2013; Facchini et al. 2016) and/or truncated due to stellar encounters (e.g., Clarke & Pringle 1993; Ostriker 1994; Olczak et al. 2006; Portegies Zwart 2016; Concha-Ramírez et al. 2019), which in turn modifies the properties of the disks and ultimately causes different outcome of planet formation; second: after the planet formation process (Phase 2), planets are no longer protected by the damping of the gaseous disks, and their orbital inclinations and eccentricities can be excited or even ejected by stellar flybys. Planetary systems in the dense regions of the cluster have lower chances to survive (Spurzem et al. 2009; Hao et al. 2013; Li & Adams 2015; Cai et al. 2017; van Elteren et al. 2019). Moreover, surviving planets from high-density regions tend to have relatively high mean eccentricities and inclinations due to their stellar encounter histories (Cai et al. 2018). Planet-planet scattering (e.g., Raymond et al. 2009) and secular resonance (e.g., Rivera & Lissauer 2001) continue long after the cluster dissolves or the planetary system leaves the cluster (Phase 3). The field exoplanets observed nowadays are the surviving planets in this natural selection process; their diversity is therefore in part shaped by their diverse birth environments in the parental cluster.

The primary objective of this paper is to study the dynamical stability and orbital architectures of planetary systems in dense YMCs, and to constrain the dynamical fates of planets in YMCs after their ejections. This paper is organized as follows: the modeling approach and the initial conditions are presented in Section 2, the results are presented in Section 3, followed by discussions in Section 4. Finally, the main conclusions are summarized in Section 5.

2 INITIAL CONDITIONS AND SIMULATIONS

Numerical simulations of planetary systems in YMCs are constrained by three factors: First, planetary systems are chaotic few-body systems, and therefore we need to carry out a grid of simulations that covers a certain parameter space and obtain the results statistically, rather than drawing conclusions from a single simulation; Second, direct N-body simulations with stellar evolution taken into account are generally required to collisional dynamics of YMCs, especially if the host YMC is rotating, having sub-structures, and/or is sub-virial; Third, there is a hierarchical timestepping problem when evolving planetary systems in YMCs. Due to the very different dynamical timescale (days or years in planetary systems and millions of years in star clusters), the integrator is forced to adopt very small time step to resolve the planetary systems accurately, which is prohibitively expensive for integrating the host clusters.

We develop a GPU-accelerated hybrid code to tackle these challenges. We realize that star clusters and planetary systems are very different, and that they have to be modeled with their own dedicated algorithms. We first integrate the host YMCs (without planets) using `NBODY6++GPU` (Spurzem 1999; Aarseth 2003; Wang et al. 2015b). The simulation is stored at a very high time resolution using an incremental adaptive storage scheme (Farr et al. 2012; Cai et al. 2015). The storage scheme, namely "Block time step (BTS) storage scheme", stores only the most recently updated particles, and thereby allows very high temporal resolution with reasonable file sizes. With the BTS data, we are then able to reconstruct the details of close encounters; the close encounters details are then inserted into the `IAS15` integrator (Rein & Spiegel 2015) of the planetary system dynamics code `rebound` (Rein & Liu 2012). The planetary system integrator queries the position vector of the closest neighbor at a timestep of years. Such a query is implemented by interpolating the BTS data on the GPUs (graphic processing units). The communication of perturbation data is implemented with the `AMUSE`[1] (Pelupessy et al. 2013; Portegies Zwart et al. 2013; Portegies Zwart & McMillan 2018) framework. Given that the density of YMCs is very high, especially in the cluster center, we include 5 nearest perturbers[2].

For simplicity, the initial condition of the star cluster

[1] `https://github.com/amusecode/amuse`

[2] We have performed a convergence test on the number of perturbers. We find that for a YMC like Westerlund-1, the results converges with the inclusion of 5 or more perturbers. Including 5 perturbers provides a reasonable tradeoff of accuracy and speed.

Table 1. List of exoplanet detections in star clusters, sorted chronologically according to the years of detection. DM: detection method; TS: transit; RV: radial velocity; TM: timing; Nep: Neptune-sized; M_S: Stellar mass in solar units $M_\odot$; m_p: planet mass in Jupiter units M_J; P: orbital period in days; TBC: to be confirmed; *: the system K2-136 is a binary system, and therefore there are two host-star mass components. a: orbital semi-major axis of the planet; e: orbital eccentricity of the planet; i: inclination of the planet.

Designation	m_p (M_J)	P **(days)**	M_S ($M_\odot$)	a **(au)**	e	i [deg]	**DM**	**Cluster**	**Ref.**‡
K2-264 b	sub-Nep	5.84	0.471	0.05	0	88.9	TS	Praesepe (M44)	[1][2]
K2-264 c	sub-Nep	19.66	0.471	0.11	0	89.6	TS	Praesepe (M44)	[1][2]
K2-231 b	0.0227	13.84	1.01	–	–	88.6	TS	Ruprecht 147	[3]
K2-136 b	super-Earth	7.98	0.74/0.1*	–	0.1	89.3	TS	Hyades	[4]
K2-136 c	super-Earth	17.3	0.74/0.1*	–	0.13	89.6	TS	Hyades	[4][5]
K2-136 d	super-Earth	25.58	0.74/0.1*	–	0.14	89.4	TS	Hyades	[4]
SAND978 b	2.18	511.2	1.37	–	–	–	RV	M67	[6]
EPIC 211913977 b	sub-Nep	14.68	0.8	–	0.1	89.4	TS	Praesepe (M44)	[7]
EPIC 211970147 b	super-Earth	9.92	0.77	–	0.1	–	TS	Praesepe (M44)	[8]
YBP401 b	0.46	4.09	1.14	–	0.15	–	RV	M67	[9]
Pr 0211 c	7.95	5 300	0.935	5.8	0.7	–	RV	Praesepe (M44)	[10]
K2-95 b	1.67	10.13	0.43	0.065	0.16	89.3	TS	Praesepe (M44)	[8][20]
EPIC 211969807 b	sub-Nep	1.97	0.51	–	0.18	88	TS	Praesepe (M44)	[8]
EPIC 211822797 b	sub-Nep	21.17	0.61	–	0.18	89.5	TS	Praesepe (M44)	[8]
K2-100 b	sub-Nep	1.67	1.18	–	0.24	85.1	TS	Praesepe (M44)	[8]
K2-77 b	1.9	8.2	0.8	–	0.14	88.7	TS	Praesepe (M44)	[11]
EPIC 211901114 b (TBC)	< 5	1.64	0.46	–	–	–	TS	Praesepe (M44)	[8]
EPIC 210490365 b	< 3	3.48	0.29	–	0.27	88.3	TS	Hyades	[12]
SAND 364 b	1.54	121.7	1.35	–	0.35	–	RV	M67	[13]
YBP1194 b	0.34	6.96	1.01	–	0.24	–	RV	M67	[13]
YBP1514 b	0.4	5.11	0.96	–	0.39	–	RV	M67	[13]
HD 285507 b	0.92	6.08	0.73	0.073	0.086	–	RV	Hyades	[14]
Kepler-66 b	0.047	17.82	1.04	0.135	–	–	TS	NGC6811	[15]
Kepler-67 b	0.047	15.73	0.87	0.12	–	–	TS	NGC6811	[15]
Pr 0201 b	0.54	4.33	1.234	–	–	–	RV	M44	[16]
Pr 0211 b	1.88	2.15	0.935	0.03	0.017	–	RV	M44	[16]
eps Tau b	7.34	595	2.70	1.9	0.15	–	RV	Hyades	[17]
NGC 2423 3 b	10.6	714	2.40	2.1	0.21	–	RV	NGC2423	[18]
NGC 4349 127 b	19.8	678	3.90	2.38	0.19	–	RV	NGC4349	[18]
PSR B1620-26 (AB) b	2.50	36 525	1.35	23	–	–	TM	M4	[19]

‡ References: [1] Rizzuto et al. (2018); [2] Livingston et al. (2019); [3] Curtis et al. (2018); [4] Mann et al. (2018); [5] Ciardi et al. (2018); [6] Brucalassi et al. (2017); [7] Mann et al. (2017a); [8] Mann et al. (2017b); [9] Brucalassi et al. (2016); [10] Malavolta et al. (2016); [11] Gaidos et al. (2017); [12] Mann et al. (2016); [13] Brucalassi et al. (2014); [14] Quinn et al. (2014); [15] Meibom et al. (2013); [16] Quinn et al. (2012); [17] Sato et al. (2007); [18] Lovis & Mayor (2007); [19] Backer et al. (1993); [20] Obermeier et al. (2016).

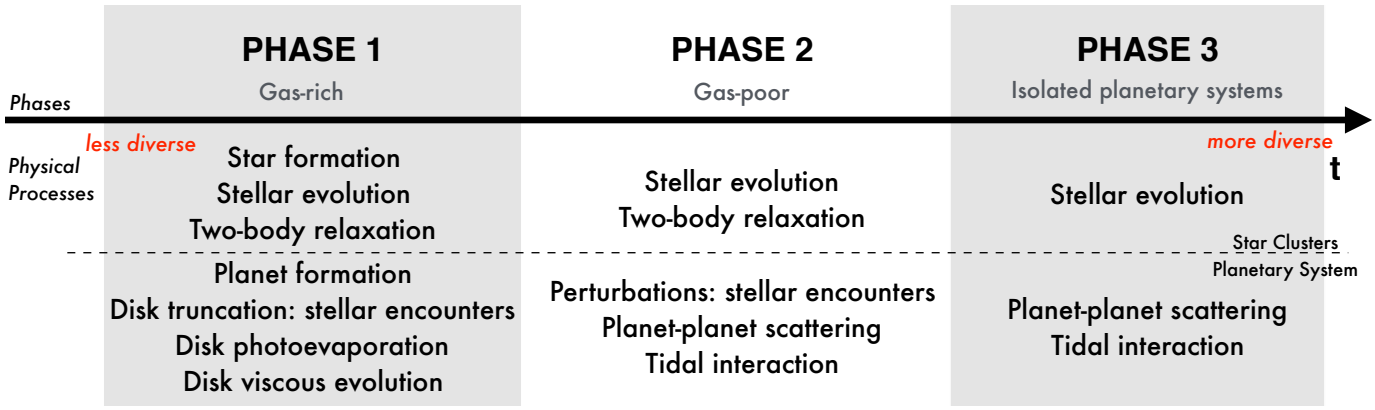

Figure 2. The coevolution of planetary systems in (massive) star clusters can be roughly divided into three phases. The diversity of exoplanets emerges gradually as a function of time.

is sampled from an $N = 128$k Plummer model (Plummer 1911) in virial equilibrium (i.e. $Q = 0.5$) with a Kroupa (2001) initial mass function. We consider the mass range of stars from $0.08M_\odot$ to $100M_\odot$. The mean stellar mass is $0.58M_\odot$. We assume 10% of primordial binaries, but assume that all planets are orbiting single stars. The binary population has a thermal eccentricity distribution. The logarithmic of semi-major axes of binaries distribute uniformly from in the range of $[3.5 \times 10^{-8}, 3.5 \times 10^{-4}]$ parsec (0.007-72 au). The two member stars of a binary system is equal-mass. The cluster is subject to the Galactic tidal field in the Solar neighborhood. The star cluster has an initial virial radius of $R_{\rm vir} = 1.74$ parsec, which is comparable to Westerlund-1 (Portegies Zwart et al. 2010). A more realistic set of YMC initial conditions that include substructures and non-virial equilibrium states will be addressed in an upcoming study.

The diversity of exoplanets clearly shows that there is no "typical" architecture for planetary systems. A planetary system may have multiple super-Earths or mini-Neptune packed in densely populated orbits (resembles the Kepler-11 system, see Lissauer et al. 2011), or it may have a lot of nearly massless objects spreading over a range of semi-major axis (e.g., the Kuiper belt). Inspired by these two distinctively different systems, we construct following two models of idealized planetary systems:

- **Model-A:** Massless multi-planet system: the system consists of 50 test particles. The semi-major axes of these planets range from 6 au to 400 au. In this model, external perturbations due to stellar flybys play an exclusive role in shaping the orbits of the test particles.
- **Model-B:** Equal-mass multi-planet system: the system consists of 5 equal-mass planets, each of which is $3M_\oplus$, separated with 15 mutual Hill Radii with the adjacent planet. The innermost planet has an initial semi-major axis of 0.5 au, and the outermost planet has an initial semi-major axis of 6 au. The system is stable without external perturbations, but its stability can be hampered when the planets are excited to higher eccentricities due to stellar flybys. In this model, we would like to study the combined effect of external perturbation and internal planet-planet scattering.

We create an ensemble of 200 identical realizations of each model and place them randomly around Solar-type stars (i.e., $1M_\odot$) in the host cluster, which results in 400 simulations. Each simulation is carried out for a timescale of 100 Myr.

3 RESULTS

3.1 Surviving Orbital Architectures

We obtain statistical results from the simulation ensembles. The evolution of planetary systems in star clusters can be considered as a natural selection process, in the sense that only those planetary systems with suitable orbital architectures will be able to survive until the end of the simulations. Since Model-A surveys a wide range of semi-major axes from 6-350 au, we are able to obtain a relatively smooth distribution of survival rates as a function of initial semi-major axes, as shown in Fig. 3. As intuitively expected, exoplanets with larger initial semi-major axes are more prone to excitation and ejections. The survival rate decreases sharply with the increment of the semi-major axis. The profile of surviving rates as a function of $\log_{10}(a_0)$ can be fitted with a linear decay function. The best fit yields:

$$f_{\rm surv}(a_0) = -0.33 \log_{10}(a_0) + 0.99. \quad (1)$$

Here, a_0 is in the unit of au. For simplicity, we could round up the constant "0.99" to 1. Ignoring planet-planet scattering, for a planet with a semi-major axis of ~ 30 au (comparable to Neptune's semi-major axis), the probability for it to be ejected is more than 0.5; the probability for a wide planet of $a > 300$ au to survive in a YMC is nearly zero. In the planetary systems where planet-planet scattering is important, we expect that an lower $f_{\rm surv}(a_0)$ (cf. Cai et al. 2017). In this sense, the exoplanets listed in Table 1, most of which being short-period planets, are not entirely due to observational biases, because long-period planets indeed have difficulties to survive in dense clusters. However, the survivability can be enhanced by tidal damping at the perihelion of a highly eccentricity orbit, causing the planet to significantly shrink its orbital semi-major axis and become a short-period planet (Shara et al. 2016).

Recently, Portegies Zwart & Jílková (2015) and Cai et al. (2018) suggest that the orbital architecture of surviving planetary systems (in the field) can be used to constraint its birth environments. Inspired by this idea, in Fig. 4 we plot the survival rate matrix as a function of both initial semi-major axis and the mean stellar density in the vicinity of the planetary system[3]. The stellar mass density of the host YMC is defined according to the Plummer density profile (e.g., Spitzer 1987):

$$\rho(r_i) = \left(\frac{3M}{4\pi a_{\rm P}^3}\right)\left(1 + \frac{r_i^2}{a_{\rm P}^2}\right)^{-5/2}, \quad (2)$$

where r is the distance between the perturbed planetary system and the cluster center, M is the total mass of the cluster, and $a_{\rm P}$ is the Plummer scale length. A time series of $r_i, i = 1, 2, 3, ...$ is obtained through the YMC simulation using `NBODY6++GPU`, and the mean stellar density is therefore calculated by averaging over the corresponding $\rho(r_i)$. In the limit of high mean stellar densities (at the top of the figure), the planetary system spends most of its time in the dense cluster center, and the system suffers from almost total ejection regardless of the initial semi-major axis. Planetary systems slightly outside the dense regions are allowed to survive provided that the initial semi-major axis is sufficiently small. In the outskirts of the cluster, even wide planets have fair chances to survive. However, we notice that the number of planetary systems in very high or very low mean stellar densities are small, and therefore we advise the readers not to extrapolate the data in this two regimes with low-number statistics. Interestingly, the constant $f_{\rm eject}$ curve,

[3] We realize that the host star may reach various regions in the cluster with different stellar densities, and averaging the stellar density alone its trajectory will lose information about the detailed dynamical history during its life time. Nevertheless, the density of a Plummer sphere grows exponentially inside the half-mass radius, and therefore integrating the density over time does provide insight into the stellar environment in which a planetary system is most affected by.

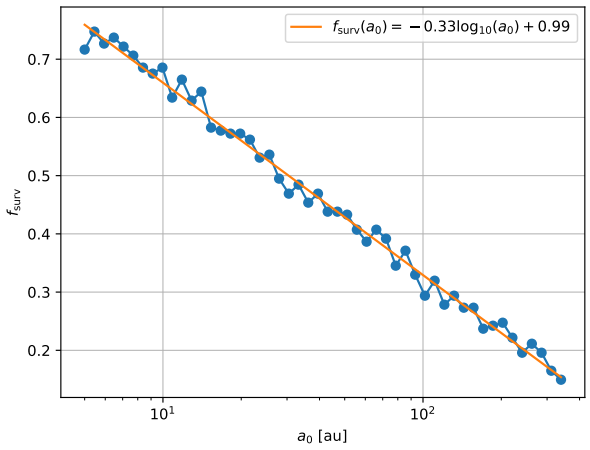

Figure 3. Survival probability of planets in YMCs as a function of the initial semi-major axes. The simulation results are shown with dots, and the fitting is shown with a line.

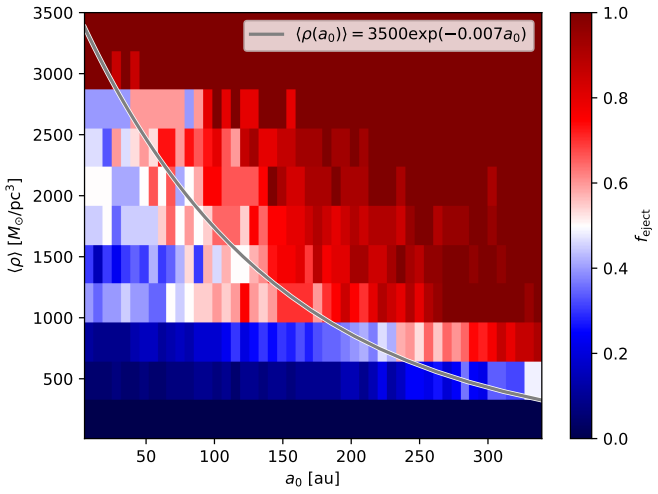

Figure 4. Survivability matrix of planets in YMCs as a function of the initial semi-major axes a_0 and the mean stellar density $\bar{\rho}$ in the vicinity of the host star. Note that there are very few planetary systems with very high or very low $\bar{\rho}$, and so the top region and the bottom regions of this figure suffers from small-number statistics. The grey curve roughly correspond to the $\langle\rho\rangle - a_0$ relation in which the ejection rate is constant (i.e. $f_{\rm eject} = 0.5$).

plotted with a grey line in Fig. 4, can be roughly approximated with an exponential decay function. In the case of $f_{\rm eject} = 0.5$, which means half of the planets are ejected, the $\langle\rho\rangle - a_0$ relation is roughly

$$\langle\rho\rangle(a_0) = 3500\exp(-0.007a_0). \quad (3)$$

Here, $\langle\rho\rangle$ is in the units of $M_\odot/{\rm pc}^3$.

For the surviving planets of both Model-A and Model-B systems, the mean orbital eccentricities and the standard deviation of eccentricities are shown in Fig. 5. The figure es-

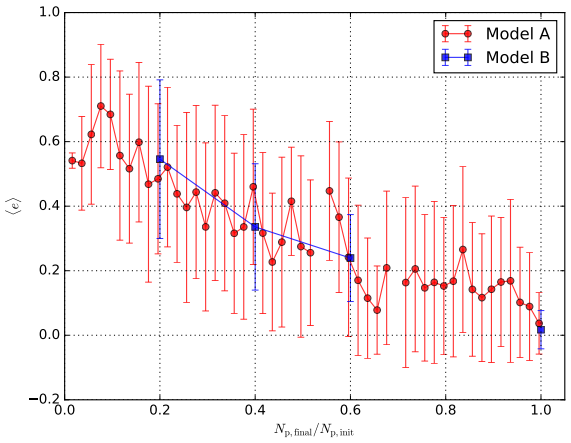

Figure 5. The mean eccentricity and the standard deviation of eccentricities (shown as errorbars) as functions of the fraction of surviving planets ($N_{\rm p,final}/N_{\rm p,init}$). The discontinuities are due to the lack of planetary systems. The climbing trend in the far-left of the plot is due to small-number statistics. Note that the error bars show the magnitudes of the standard deviation of eccentricities, and therefore the negative values in the lower parts of some error bars do not mean negative eccentricities.

sentially states that if a planetary system manages to retain $N_{\rm p}$ planets in the star cluster (at the end of the simulation), its mean orbital eccentricity should not be higher than the value given at the central point of the error bar. For instance, in order for all planets in a planetary system to survive, the system must be largely "untouched" by stellar encounters such that the mean eccentricity is of the order of $\langle e\rangle \sim 0.05$. Similarly, Fig. 6 shows the mean inclinations (and their standard deviations) as a function of $N_{\rm p}$. The inclinations are measured with respect to the primordial orbital plane of the planetary systems when the simulations start. Indeed, the multiplicity function exhibits anti-correlation with the dynamical temperature of the system: hotter systems have a lesser degree of multiplicity, whereas cooler systems have higher degrees of multiplicity. As a consequence of angular momentum exchanges, Model-A systems have slightly smaller $\langle e\rangle$ and $\langle i\rangle$ but larger standard deviation compared to Model-B.

3.2 Survival Rates as a Function of Time and Initial Semi-major Axes

It is clear from the previous subsection that initial semi-major axes matter to the survival rates. Now we can consider the time-dependence. The profiles of survival rates as a function of time for Model-A systems and Model-B systems are plotted in Fig. 7 and Fig. 8, respectively. The survival rate drops rapidly during the first few Myr (especially those wide planets in Model-A), and then the decline becomes more gradual in due time. Again, the natural selection process provides a feasible explanation to this behavior: a large number of planets are eliminated in the beginning since they are unfit in dense stellar environments, but the more resilient ones prevail. In due time, the ejection rates become increasingly gradual since the surviving planets are more difficult to

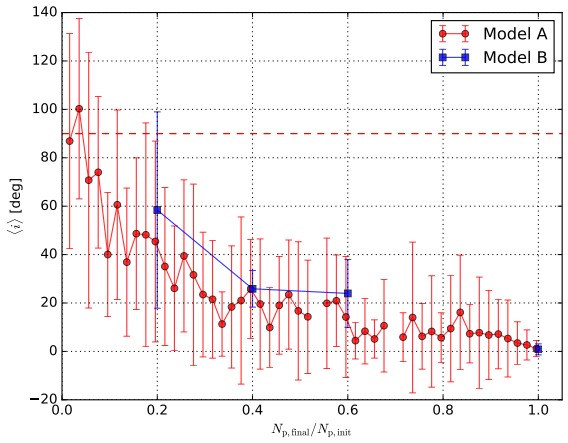

Figure 6. The mean inclinations and the standard deviation of inclinations (shown as errorbars) as functions of the fraction of surviving planets. Notation same as Fig. 5. Note that the error bars show the magnitudes of the standard deviation of inclinations, and therefore the negative values in the lower parts of some error bars do not mean negative inclinations.

Table 2. Fitted coefficients of $f_{\rm surv}(t, a_0)$ for Model-A systems, where t is in the unit of Myr and a_0 is in the unit of au.

i	α_i	β_i	γ_i
1	-3.1×10^{-6}	0.0023	0.2
2	-6.5×10^{-7}	6.8×10^{-5}	-0.023
3	2.5×10^{-6}	-0.0024	0.78

eject. As such, the remaining planets at the end of the simulations generally reveal the suitable orbital architectures for surviving in dense stellar environments. The planets in Model-A with a wide range of initial semi-major axes generates a series of decay profiles, which can be fitted well with a family of functional form of exponential decay:

$$f_{\rm surv}(t, a_0) = g_1(a_0) \exp(-g_2(a_0)t) + g_3(a_0), \quad (4)$$

where a_0 is the initial semi-major axis, and g_1, g_2, and g_3 are three second-order polynomials defined as:

$$g_i(a_0) = \alpha_i a_0^2 + \beta_i a_0 + \gamma_i, \quad (5)$$

with $i = 1, 2, 3$. The coefficient of the fitting is listed in Table 2.

Due to the planet-planet scattering process in Model-B systems, external perturbations is no longer the sole driver of planet ejections. It is interesting to notice in Fig. 8 that the innermost planet is not necessarily the ones that have the highest chance to survive. This result is in agreement with an earlier study by Cai et al. (2017), where they simulated smaller clusters of $N = 2000, 8000, 32000$ stars.

3.3 Kinematics of Free-Floating Planets

Should a planet be ejected due to the perturbation of stellar encounters, a natural question arises regarding its destination: is the planet going to wander inside the host cluster, or

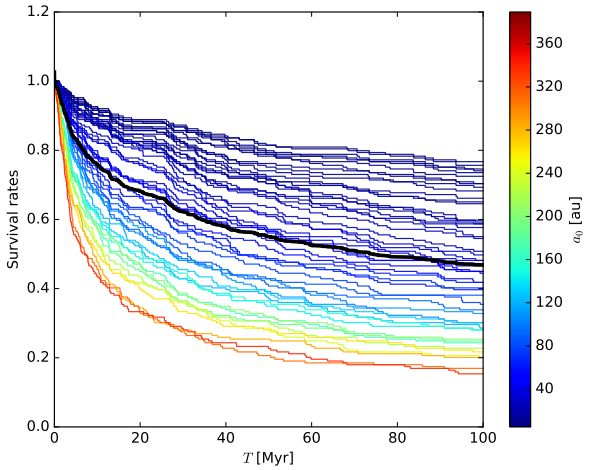

Figure 7. Survival rates of individual planets in YMCs as a function of time (Model-A). The initial semi-major axes of planets a_0 are encoded in colors. The thick black curve corresponds to the overall survival rates, which is defined as $N_{\rm p,final}/N_{\rm p,init}$. The uppermost curve generally corresponds to the innermost planet (which, in turn, corresponds to the leftmost part of Fig. 3), and the lowermost curve generally corresponds to the outermost planet (corresponds to the rightmost part of Fig. 3).

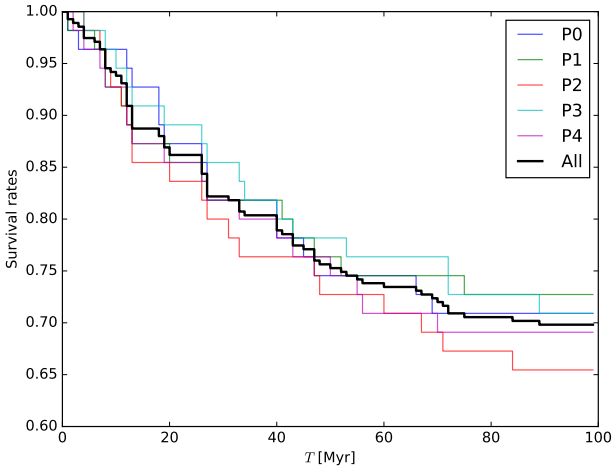

Figure 8. Survival rates of individual planets in YMCs as a function of time (Model-B). P0 is the innermost planet with an initial semi-major axis of 0.5 au, and P5 is the outermost planet in this model with an initial semi-major axis of 6 au.

is it going to escape from the cluster? In Fig. 9, we plot the ejection speeds of free-floating planets as a function of their semi-major axis immediately prior to the ejection ($a_{\rm eject}$). The initial semi-major axes at $t = 0$ are shown in colors. The ejection speeds are scaled to the escape velocity of the Plummer sphere at the point of ejection (Heggie & Hut 2003):

$$v_{\rm esc,sc}(r) = \left(\frac{2GM}{r}\right)^{1/2} \left(1 + \frac{r_{\rm hm}^2}{r^2}\right)^{-3/4}, \quad (6)$$

where r is the distance from the planet ejection location to the host cluster center, $r_{\rm hm}$ is the half-mass radius of the cluster, G is gravitational constant, and M is the total mass of the cluster.

It is evident from Fig. 9 that high ejection velocities are produced from planets with smaller $a_{\rm eject}$, where the orbital velocities are higher. There are two ejection velocity regimes: within the shaded area, the ejected planet has sufficient velocity to escape from the cluster, and therefore once they are ejected from their planetary systems, they are also instantaneously become unbound to the cluster potential; below the line, the planets only have enough velocity to escape from their planetary systems, but they do not have sufficient velocity to escape from the host cluster, and therefore they will be free-floating planets inside the cluster. About 1/3 ($\sim$ 28.8%) of ejected planets have sufficient speeds to escape from the host cluster immediately. This population, namely "prompt ejectors", mostly originate from the inner planetary systems with small semi-major axes. More than 2/3 of ejected planets ($\sim$ 71.2%) are the so-called intra-cluster free-floating planets, which, due to their low masses, may be subsequently expelled from the host cluster through the mass-segregation process that takes place at a timescale of $\sim$ 200 Myr for the YMC model used in our simulations (Spitzer & Hart 1971; Portegies Zwart et al. 2006, 2010).

In a recent study, Wang et al. (2015a) simulate the dynamics of free-floating planets in an $N \sim 2000$ star cluster using the GPU-accelerated direct N-body package `NBODY6` (Aarseth 2003; Nitadori & Aarseth 2012). They observe that the planet-to-star ratio drops rapidly by half in the first few Myr, and then followed by a steady and linear decline in the next 1.6 Gyr until the population of free-floating planets depletes. The authors argue that the rapid decay in the first few Myr is a consequence of direct ejections, whereas the steady decline is a result of the mass segregation process. Since the cluster tends to establish an equal-partition of energy, low-mass objects will, therefore, obtain high velocities and eventually escape host cluster. We expect a large population of free-floating planets in any galaxy. Nevertheless, it is important to note that the free-floating planet population has already existed at the beginning of the simulations in Wang et al. (2015a), where they sample the initial positions and velocities of the planets from the same distribution os that of the stars. In a new study by van Elteren et al. (2019), the free-floating planet population is generated in a more self-consistent way, as they model all planets to be initially bound to host stars, and that free-floating planets are only created upon ejections. Their simulations with a super-virial ($Q = 0.6$) and fractal ($F = 1.26$) cluster yield the prompt ejector population and the delayed ejector population as well. More interestingly, they are able to simulate the recapturing of free-floating planets. They conclude that a small fraction ($\sim$ 1.5%) of free-floating planets are subsequently recaptured by another star. Since this fraction is low, and that the recaptured planet is typically on highly eccentric and inclined wide orbits (which are prone to perturbations) (Jílková et al. 2015), we do not think that recapturing is an effective mechanism to help YMCs to retain planets.

Interestingly, we also observe that many planets (especially those with large $a_{\rm init}$) have undergone substantial outward migrations. The energy injected by stellar flybys has elevated the semi-major axes of outer planets (and even a small number of inner planets), making the planetary systems increasingly "fluffy" as a function of time. Therefore, dense stellar environments can lead to an outflow of planets/massless-particles. Planets and low-mass particles can either be ejected *in situ* at roughly their initial semi-major axes, or undergoes outward migration and subsequently be ejected at larger semi-major axes (e.g., Portegies Zwart et al. 2018).

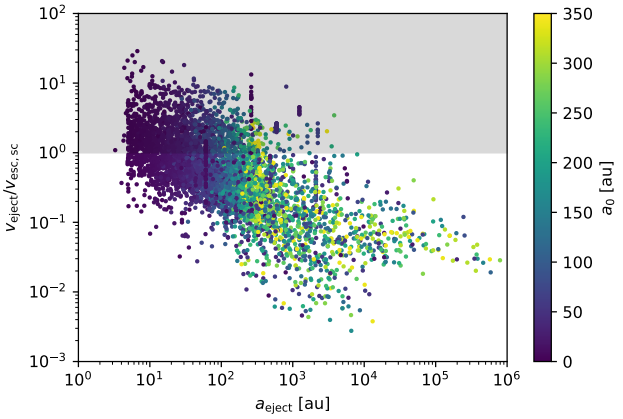

Figure 9. Ejection speed of free-floating planets normalized to the corresponding escape speed of the host cluster (at the location where the ejection takes place). The x-axis is the semi-major axis of the planets prior to their ejections. The color encodes the initial semi-major ($a_{\rm init}$) axis of ejected planets. There are two populations of free-floating planets: in the shaded area, the ejected planet has sufficient velocity to escape the host cluster immediately ($\sim$ 28.8%); below the horizontal line, the ejected planet does not have sufficient velocity to escape the host cluster ($\sim$ 71.2%).

In the planetary systems where planet-planet scattering is important (e.g. Model-B systems), the ejection of planets is not solely caused by external perturbations. A series of moderate or weak encounters may gradually increase the angular momentum deficits (Laskar 1997) of an externally perturbed planetary system, and then a planet may get ejected by another planet during a close encounter event long after the stellar encounter. Indeed, the planet ejection efficiency is roughly doubled in this "delayed ejection" scenario Cai et al. (2017).

4 DISCUSSIONS

The planet formation process, which takes place in protoplanetary disks, may be complicated by the high stellar density and intense radiation fields in YMCs. While our simulations cover a wide range of initial semi-major axes from 0.5 au to 350 au, the perspectives of planet formation in extreme environments is still under active debates. There are several dedicated studies on the effects of stellar environments to the protoplanetary disks. For example, a number of authors suggest that the protoplanetary disk can be truncated, or even disrupted by close stellar flybys (e.g., Olczak et al. 2012; Portegies Zwart 2016; Vincke & Pfalzner 2016;

Wijnen et al. 2017; Richert et al. 2018; Vincke & Pfalzner 2018), although the viscous evolution of the disk may be helpful in damping the eccentricity and eventually establishing a new equilibrium (Concha-Ramírez et al. 2019). On the other hand, the initial mass function dictates that there will be a small fraction of O/B stars that emit energetic FUV photons. Due to the proximity, these FUV photos can photoevaporate the disk (Anderson et al. 2013; Haworth et al. 2018; Winter et al. 2018), which may prematurely halt the core accretion process and the disk-driven process.

It is worthy to mention that the structure of the YMC is evolving quickly due to the gas expulsion (e.g., Goodwin & Bastian 2006; Baumgardt et al. 2008; Krause et al. 2016). Once the intra-cluster gas is gone, the cluster becomes supervivial temporarily, and the subsequent reestablishment of virial equilibrium may lead to a temporary surge of planet ejection rates. In a recent study, Zheng et al. (2015) carry out direct N-body simulations of clusters with different initial morphologies and initial virial states. They conclude that non-equilibrium conditions in host clusters can indeed boost the ejection rate, and that for a cluster of $N = 1000$ stars, a virial equilibrium is reestablished at an energy equal-partition timescale of 5 Myr, after which the ejection rates becomes steady again.

Given the high stellar density, it is possible that an ejected planet can be recaptured by another star. Perets & Kouwenhoven (2012) suggest that if recapturing does happen, planets are likely to be captured into wide orbits with the new semi-major axes of the order of $10^2 - 10^6$ au. In this sense, the probability for the recaptured planet to stay bound to its new planetary system depends on how long the new planetary system stays in the host YMC. If the new planetary system stays in the YMC for an extensive period of time, the chances of getting re-ejection would be high. However, if the new planetary system has already escaped from the host YMC, then the recaptured planet may be able to stay bound over secular timescale. In a related study, Jílková et al. (2015) suggest that the dwarf planet Sedna in the Solar System, as we as many Sednitos, may be a result of recapturing. In a related study, Malmberg et al. (2011) suggest another scenario where up to a few percent of low-mass intruders may themselves be captured and become bound to the host star, which can potentially lead to drastic changes in the orbital properties of the planets orbiting the stars.

According to the planet-metallicity correction (Fischer & Valenti 2005), the GC environment, which is typically metal-poor, is not ideal for the formation of Jovian planets. However, the formation of terrestrial planets is less affected by the metallicity (Wang & Fischer 2015). In this sense, we suspect that the lack of planet detection in dense GCs such as 47 Tuc (Gilliland et al. 2000; Masuda & Winn 2017) is in fact due to the low frequency of the more-easily detectable Jovian planets. We speculate that short-period terrestrial planets can be found in dense GCs with next-generation surveys.

5 CONCLUSIONS

Young mass star clusters (YMCs) may be the progenitor of globular clusters (GCs). In this study, we address two fundamental problems regarding whether YMCs can harbor planets and whether GCs can inherit planets from YMCs. We model the dynamical evolution of planetary systems in YMCs using direct N-body simulations in the `AMUSE` framework. Our main conclusions are summarized below:

- The dense stellar environments in YMCs do have profound effects in shaping planetary systems. Nascent planetary systems are forced into a natural selection process, and that only the most robust orbital architectures can survive. Dense stellar environments favor planets with short orbital periods, and the survival probability as a function of the initial semi-major axis a_0 (in astronomical units) can be estimated with $f_{\rm surv}(a_0) = -0.33 \log_{10}(a_0) + 1$. On average, the survival rates for planets with semi-major axes larger than 20 au is lower than 50% after the 100 Myr evolution. With a fixed $f_{\rm surv} = 0.5$, the mean stellar density (in the units of $M_\odot/{\rm pc}^3$) roughly scales with the a_0 as $\langle\rho(a_0)\rangle = 3500\exp(-0.007a_0)$, indicating that only planets with very tight orbits can survive in the dense regions of the host cluster.
- Planetary systems with high multiplicity can only be found in the outskirts of YMCs or in the field. In contrast, the dense cluster center produces "hot" planetary systems with low-degree of multiplicity and high mean eccentricities/inclinations. The host cluster shapes its planetary system through a natural selection process in that only the most suitable orbital architectures survive, and the survivability of planets as a function of time can be well approximated with an exponential decay function.
- Weak stellar encounters produce "cluster wanderers", whereas strong encounters produce "cluster escapers". Among those free-floating planets (FFPs) produced by dynamical ejections, $\sim 28.8\%$ of them have sufficient velocities to escape from the host clusters. These cluster escapers are mostly originated from the inner regions of the original planetary systems where the orbital speeds are high. Ejecting these short-period planets requires strong encounters, which are rare events. The prevalence of medium-to-weak encounters is only able to eject wide planets, whose low orbital velocities will cause them to be confined in the host clusters. However, "cluster wanderers" may be gradually expelled by the subsequent mass-segregation process in the host cluster.
- Free-floating planets (FFPs) in the Galactic field can be generated through four channels: (1) direct ejection from the inner regions of the original planetary systems through strong encounters; (2) ejected from the original planetary systems while remaining bound to the cluster, until being expelled by the mass-segregation process; (3) ejected from the original planetary systems and remain bound to the cluster until the dissolution of the host clusters; (4) ejected directly from an isolated planetary systems in the Galactic field, whose angular momentum deficit was stirred up by stellar encounters when the planetary systems were still in the host cluster.

Our results show that short-period planets can survive in YMCs. However, GCs are unlikely to inherit free-floating planets from their YMC siblings, due to the efficiency of the mass segregation process operating on "cluster wanderers" in YMCs. We speculate that the lack of planet detection in dense GCs is actually due to the lack of Jovian planets in metal-poor environments, and therefore short-period

terrestrial planets can still be found in dense GCs with next-generation surveys.

ACKNOWLEDGEMENTS

We thank Ignas Snellen for an insightful discussion. This project is supported by SURFsara (Dutch national supercomputing facility) through the SOIL (SURFsara Open Innovation Lab) initiative and the EU Horizon 2020 project COMPAT (grant agreement No. 671564). The simulations are carried out on the supercomputer `Cartesius` and the LGM-II GPU machine (NWO grant #621.016.701). M.B.N.K. acknowledges support from the National Natural Science Foundation of China (grant 11573004). This research was supported by the Research Development Fund (grant RDF-16-01-16) of Xi'an Jiaotong-Liverpool University (XJTLU). We acknowledge the support of the DFG priority program SPP 1992 "Exploring the Diversity of Extrasolar Planets (Sp 345/20-1)". This project makes use of the SAO/NASA Astrophysics Data system and the `exoplanet.eu` database.

REFERENCES

Aarseth S. J., 2003, Gravitational N-Body Simulations
Adams F. C., 2010, Annual Review of Astronomy and Astrophysics, 48, 47
Adams F. C., Proszkow E. M., Fatuzzo M., Myers P. C., 2006, ApJ, 641, 504
Anderson K. R., Adams F. C., Calvet N., 2013, ApJ, 774, 9
Armitage P. J., 2000, A&A, 362, 968
Backer D. C., Foster R. S., Sallmen S., 1993, Nature, 365, 817
Baumgardt H., Kroupa P., Parmentier G., 2008, MNRAS, 384, 1231
Brucalassi A., et al., 2014, A&A, 561, L9
Brucalassi A., et al., 2016, A&A, 592, L1
Brucalassi A., et al., 2017, A&A, 603, A85
Cai M. X., Meiron Y., Kouwenhoven M. B. N., Assmann P., Spurzem R., 2015, ApJS, 219, 31
Cai M. X., Kouwenhoven M. B. N., Portegies Zwart S. F., Spurzem R., 2017, MNRAS, 470, 4337
Cai M. X., Portegies Zwart S., van Elteren A., 2018, MNRAS, 474, 5114
Ciardi D. R., et al., 2018, AJ, 155, 10
Clarke C. J., Pringle J. E., 1993, MNRAS, 261, 190
Concha-Ramírez F., Vaher E., Portegies Zwart S., 2019, MNRAS, 482, 732
Curtis J. L., et al., 2018, AJ, 155, 173
Facchini S., Clarke C. J., Bisbas T. G., 2016, MNRAS, 457, 3593
Farr W. M., et al., 2012, New Astron., 17, 520
Fedele D., van den Ancker M. E., Henning T., Jayawardhana R., Oliveira J. M., 2010, A&A, 510, A72
Fischer D. A., Valenti J., 2005, ApJ, 622, 1102
Ford E. B., Joshi K. J., Rasio F. A., Zbarsky B., 2000, ApJ, 528, 336
Gaidos E., et al., 2017, MNRAS, 464, 850
Gilliland R. L., et al., 2000, ApJ, 545, L47
Goodwin S. P., Bastian N., 2006, MNRAS, 373, 752
Hao W., Kouwenhoven M. B. N., Spurzem R., 2013, MNRAS, 433, 867
Haworth T. J., Clarke C. J., Rahman W., Winter A. J., Facchini S., 2018, MNRAS, 481, 452
Heggie D., Hut P., 2003, The Gravitational Million-Body Problem: A Multidisciplinary Approach to Star Cluster Dynamics
Jílková L., Portegies Zwart S., Pijloo T., Hammer M., 2015, MNRAS, 453, 3157
Krause M. G. H., Charbonnel C., Bastian N., Diehl R., 2016, A&A, 587, A53
Kroupa P., 2001, MNRAS, 322, 231
Kruijssen J. M. D., 2014, Classical and Quantum Gravity, 31, 244006
Lada C. J., Lada E. A., 2003, Annual Review of Astronomy and Astrophysics, 41, 57
Laskar J., 1997, A&A, 317, L75
Li G., Adams F. C., 2015, MNRAS, 448, 344
Lissauer J. J., et al., 2011, Nature, 470, 53
Livingston J. H., et al., 2019, MNRAS, 484, 8
Longmore S. N., et al., 2014, Protostars and Planets VI, pp 291–314
Lovis C., Mayor M., 2007, A&A, 472, 657
Malavolta L., et al., 2016, A&A, 588, A118
Malmberg D., de Angeli F., Davies M. B., Church R. P., Mackey D., Wilkinson M. I., 2007, MNRAS, 378, 1207
Malmberg D., Davies M. B., Heggie D. C., 2011, MNRAS, 411, 859
Mann A. W., et al., 2016, ApJ, 818, 46
Mann A. W., et al., 2017a, AJ, 153, 64
Mann A. W., et al., 2017b, AJ, 153, 64
Mann A. W., et al., 2018, AJ, 155, 4
Masuda K., Winn J. N., 2017, AJ, 153, 187
Meibom S., et al., 2013, Nature, 499, 55
Nitadori K., Aarseth S. J., 2012, MNRAS, 424, 545
Obermeier C., et al., 2016, AJ, 152, 223
Olczak C., Pfalzner S., Spurzem R., 2006, ApJ, 642, 1140
Olczak C., Kaczmarek T., Harfst S., Pfalzner S., Portegies Zwart S., 2012, ApJ, 756, 123
Ostriker E. C., 1994, ApJ, 424, 292
Parker R. J., Quanz S. P., 2012, MNRAS, 419, 2448
Pelupessy F. I., van Elteren A., de Vries N., McMillan S. L. W., Drost N., Portegies Zwart S. F., 2013, A&A, 557, A84
Perets H. B., Kouwenhoven M. B. N., 2012, ApJ, 750, 83
Plummer H. C., 1911, MNRAS, 71, 460
Portegies Zwart S. F., 2016, MNRAS, 457, 313
Portegies Zwart S. F., Jílková L., 2015, MNRAS, 451, 144
Portegies Zwart S., McMillan S., 2018, Astrophysical Recipes; The art of AMUSE, doi:10.1088/978-0-7503-1320-9.
Portegies Zwart S. F., Baumgardt H., McMillan S. L. W., Makino J., Hut P., Ebisuzaki T., 2006, ApJ, 641, 319
Portegies Zwart S. F., McMillan S. L. W., Gieles M., 2010, ARA&A, 48, 431
Portegies Zwart S., McMillan S. L. W., van Elteren E., Pelupessy I., de Vries N., 2013, Computer Physics Communications, 184, 456
Portegies Zwart S., Torres S., Pelupessy I., Bédorf J., Cai M. X., 2018, MNRAS, 479, L17
Proszkow E.-M., Adams F. C., 2009, The Astrophysical Journal Supplement Series, 185, 486
Quinn S. N., et al., 2012, ApJ, 756, L33
Quinn S. N., et al., 2014, ApJ, 787, 27
Raymond S. N., Barnes R., Veras D., Armitage P. J., Gorelick N., Greenberg R., 2009, ApJ, 696, L98
Rein H., Liu S. F., 2012, A&A, 537, A128
Rein H., Spiegel D. S., 2015, MNRAS, 446, 1424
Richert A. J. W., Getman K. V., Feigelson E. D., Kuhn M. A., Broos P. S., Povich M. S., Bate M. R., Garmire G. P., 2018, MNRAS, 477, 5191
Rivera E. J., Lissauer J. J., 2001, ApJ, 558, 392
Rizzuto A. C., Vanderburg A., Mann A. W., Kraus A. L., Dressing C. D., Agüeros M. A., Douglas S. T., Krolikowski D. M., 2018, AJ, 156, 195
Sato B., et al., 2007, ApJ, 661, 527
Shara M. M., Hurley J. R., Mardling R. A., 2016, ApJ, 816, 59

Sigurdsson S., Richer H. B., Hansen B. M., Stairs I. H., Thorsett S. E., 2003, Science, 301, 193
Spitzer L., 1987, Dynamical evolution of globular clusters
Spitzer Jr. L., Hart M. H., 1971, ApJ, 166, 483
Spurzem R., 1999, Journal of Computational and Applied Mathematics, 109, 407
Spurzem R., Giersz M., Heggie D. C., Lin D. N. C., 2009, ApJ, 697, 458
Störzer H., Hollenbach D., 1999, ApJ, 515, 669
Vincke K., Pfalzner S., 2016, ApJ, 828, 48
Vincke K., Pfalzner S., 2018, ApJ, 868, 1
Wang J., Fischer D. A., 2015, AJ, 149, 14
Wang L., Kouwenhoven M. B. N., Zheng X., Church R. P., Davies M. B., 2015a, MNRAS, 449, 3543
Wang L., Spurzem R., Aarseth S., Nitadori K., Berczik P., Kouwenhoven M. B. N., Naab T., 2015b, MNRAS, 450, 4070
Wijnen T. P. G., Pols O. R., Pelupessy F. I., Portegies Zwart S., 2017, A&A, 604, A91
Winn J. N., Fabrycky D. C., 2015, ARA&A, 53, 409
Winter A. J., Clarke C. J., Rosotti G., Ih J., Facchini S., Haworth T. J., 2018, MNRAS, 478, 2700
Zheng X., Kouwenhoven M. B. N., Wang L., 2015, MNRAS, 453, 2759
van Elteren A., Portegies Zwart S., Pelupessy I., Cai M., McMillan S., 2019, arXiv e-prints, p. arXiv:1902.04652

This paper has been typeset from a TEX/LATEX file prepared by the author.